Electronic Supplementary Material (ESI) for Nanoscale.

Supporting Information for

Integrating molecular design and crystal engineering approaches in non-humidified intermediate-temperature proton conductors based on a Dawson-type polyoxometalate and poly(ethylene glycol) derivatives

Naoki Ogiwara,[a] Masahiro Tomoda,[a] Shotaro Miyazaki,[a] Zhewei Weng,[a] Hiroshi Takatsu,[b] Hiroshi Kageyama,[b] Toshiyuki Misawa,[c] Takeru Ito,[c] and Sayaka Uchida*[a]

[a] Department of Basic Science, School of Arts and Sciences, The University of Tokyo, Komaba, Meguro-ku, Tokyo 153-8902, Japan

[b] Department of Energy and Hydrocarbon Chemistry, Graduate School of Engineering, Kyoto University, Nishikyo-ku, Kyoto 615-8510, Japan

[c] Department of Chemistry, School of Science, Tokai University, 4-1-1 Kitakaname, Hiratsuka 259-1292, Japan

Table of contents

Experimental Section

Materials.

$K_6[\alpha\text{-}P_2W_{18}O_{62}]\cdot nH_2O$ and $H_6[\alpha\text{-}P_2W_{18}O_{62}]\cdot nH_2O$ were synthesized according to previously reported methods.[1] $CsNO_3$ and polyethylene glycols were purchased from Kanto Kagaku and used as received.

Syntheses.

CsK-PEG400 was synthesized as follows: 3.0 g of PEG400 (molecular weight = 400) and 0.20 g of $CsNO_3$ were added to 5mL of H_2O (solution A). 0.25 g of $K_6[P_2W_{18}O_{62}]\cdot nH_2O$ was added to 5 mL of H_2O (solution B). Solution B was added to solution A dropwise and the mixed solution was stirred at 80 °C for 30 min. The solution was cooled overnight to room temperature, left at 5 °C for 1 day, and colorless crystals of **CsK-PEG400** were obtained. The synthetic methods were basically the same for **CsK-PGME** (PGME was used instead of PEG400), **CsK-PGDE** (PGDE was used instead of PEG400), **CsK-PEG300** (PEG300 was used instead of PEG400), **Cs-PEG200** (PEG200 was used instead of PEG400) and **Cs-PEG400** ($H_6[\alpha\text{-}P_2W_{18}O_{62}]\cdot nH_2O$ was used instead of $K_6[\alpha\text{-}P_2W_{18}O_{62}]\cdot nH_2O$, and 0.35 g of $CsNO_3$ was used instead of 0.20 g of $CsNO_3$). Anal. Found (calcd) of $Cs_{3.5}K_{1.3}H_{1.2}[\alpha\text{-}P_2W_{18}O_{62}]\cdot 4.2PEG400\cdot 3.6H_2O$ (**CsK-PEG400**): H, 1.7 (2.4); C, 13 (13); P, 0.96 (0.94); K, 0.77 (0.77); Cs, 7.1 (7.1); W, 49 (50). Anal. Found (calcd) of $Cs_{3.3}K_{1.5}H_{1.2}[\alpha\text{-}P_2W_{18}O_{62}]\cdot 4.3PGME400\cdot 2.2H_2O$ (**CsK-PGME**): H, 1.5 (2.5); C, 14 (13); P, 0.99 (0.93); K, 0.88 (0.88); Cs, 6.6 (6.6); W, 50 (50). Anal. Found (calcd) of $Cs_{3.1}K_{1.6}H_{1.3}[\alpha\text{-}P_2W_{18}O_{62}]\cdot 3.6PGDE500\cdot 3.9H_2O$ (**CsK-PGDE**): H, 1.6 (2.6); C, 14 (13); P, 1.0 (0.93); K, 0.93 (0.93); Cs, 6.2 (6.2); W, 48 (49). Anal. Found (calcd) of $Cs_{3.5}K_{1.5}H_{1.0}[\alpha\text{-}P_2W_{18}O_{62}]\cdot 5.5PEG400\cdot 3.9H_2O$ (**CsK-PEG300**) : H, 1.9 (2.4); C, 13 (13); P, 0.93 (0.93); K, 0.87 (0.87); Cs, 7.1 (7.1); W, 45 (50). Anal. Found (calcd) of $Cs_{5.0}H_{1.0}[\alpha\text{-}P_2W_{18}O_{62}]\cdot 4.3PEG200\cdot 1.2H_2O$ (**Cs-PEG200**): H, 0.45 (1.4); C, 7.2 (7.2); P, 1.1 (1.1); Cs, 11 (11); W, 53 (56). Anal. Found (calcd) of $Cs_{5.0}H_{1.0}[\alpha\text{-}P_2W_{18}O_{62}]\cdot 4.1PEG400\cdot 6.6H_2O$ (**Cs-PEG400**): H, 1.9 (2.4); C, 12 (12); P, 0.98 (0.92); Cs, 9.7 (9.7); W, 47 (49).

Single-crystal X-ray diffraction analysis.

X-ray diffraction data for **CsK-PEG400** were collected with a combination of rayonix-MX225-HS CCD area detector and a synchrotron radiation (λ = 0.61000 Å) at 2D beamline in Pohang Accelerator Laboratory (PAL). The processing of diffraction images and absrotpion correction were both performed with HKL3000.[2] X-ray diffraction data for **Cs-PEG200** were collected with a HyPix-6000 X-ray photon counting detector (Rigaku Oxford diffraction) and graphite-monochromated Mo *K*α radiation (λ = 0.71073 Å). X-ray diffraction data for **Cs-PEG400** were collected with a CCD 2-D detector using a Rigaku Saturn diffractometer and graphite monochromated Mo *K*α radiation (λ = 0.71073 Å). The structures were solved by dual-space algorithm using SHELXT (ver. 2018/2) and refined by the full-matrix least-squares method on F^2 using SHELXL (ver. 2018/3). The calculations were performed using the CrystalStructure[3] (**CsK-PEG400**) or CrysAlisPro[4] (**Cs-PEG400** and **Cs-PEG200**) package. The deposited numbers of Cambridge Crystallographic Data Centre (CCDC) are CCDC-2047152 for **CsK-PEG400**, CSD-2052968 for **Cs-PEG200**, and CSD-2052969 for **Cs-PEG400**. Void analysis was carried out by Mercury structure visualization software (CCDC) with a probe radius of 2.0 Å and approximate grid space of 0.7 Å.

Measurements.

Combustion analysis (Elementar, vario MICRO cube) was used for the quantitative analysis of C and H. Inductively coupled plasma optical emission spectrometry (ICP-OES) (Agilent Technologies, ICP-OES720) was used for the quantitative analysis of P and W. AAS analysis (Hitachi, ZA3000) was used for the quantitative analysis of K and Cs. Thermogravimetry-differential thermal analysis (TG-DTA) data were measured with a Thermo Plus 2 thermogravimetric analyzer (Rigaku Corporation) with α-Al_2O_3 as a reference under a dry N_2 and O_2 flow (80 and 20 mL min^{-1}, respectively) in the temperature range of 303−773 K at an increasing rate of 10 K min^{-1}. Powder X-ray diffraction (PXRD) patterns were measured with a New advance D8 X-ray diffractometer (Bruker) by using Cu Kα radiation (λ = 1.54056 Å, 40 kV−40 mA) at 2θ = 3−40 ° and 1.8 ° min^{-1} . Solid-state magic angle

spinning (MAS) NMR spectra (MAS rate 10 kHz) were recorded with an AVANCE 400WB spectrometer (Bruker), and the resonance frequency for ^{13}C was 100.6 MHz. Adamantane (^{13}C, 28.5 and 38. ppm) was used as an external standard for the calibration of chemical shifts. Cross-polarization (CP) was used for the NMR measurements. Alternating current (AC) impedance measurements: about 0.1 g of the compounds was compressed at 40 kgf cm^{-2} into pellets of 10 mm in diameter and ca. 0.6 mm in thickness. The pellets were cut into several pieces and used for the ac impedance measurement. AC impedance measurements were carried out in a temperature and humidity chamber with a BioLogic VMP3 multichannel potentiostat/galvanostat (Science Instruments) over the frequency range of 2 Hz to 7 MHz and ac amplitude of 500 mV. Copper electrodes were attached on both faces of the pellets. Bulk conductivities were estimated by semicircle fitting of Nyquist plots. Specific heat was measured by applying a thermal relaxation method with a commercial calorimeter (Quantum Design, PPMS) in a temperature range from 200 to 2 K.

Table S1. Crystallographic data of **CsK-PEG400**, **Cs-PEG200**, and **Cs-PEG400**

	CsK-PEG400	**Cs-PEG200**	**Cs-PEG400**
Crystal system	hexagonal	orthorhombic	monoclinic
Space group	$P6_322$ (#182)	*Pmmn* (#59)	$P2_1/c$ (#14)
Unit cell	a = 17.2090(3) c = 28.5570(5)	a = 24.1713(15) b = 16.5887(9) c = 12.6541(6)	a = 17.261(5) b = 30.571(8) c = 28.331(8) β = 105.688(8)
Volume	7324.1(3)	5073.9(3)	14393(7)
Z	2	2	4
D_{calc} (g cm^{-3})	2.168	3.291	2.320
F(000)	4087	4266	8532
h, k, l range	–24/25, –19/19, –39/39	–29/29, –17/20, –15/14	–20/20, –36/34, –33/33
μ (mm^{-1})	9.286	22.174	15.633
$R_1(I > 2\sigma(I))$	0.1008	0.0969	0.1740
wR_2 (all data)	0.3674	0.2956	0.4733
GOF on F^2	1.057	1.049	1.582

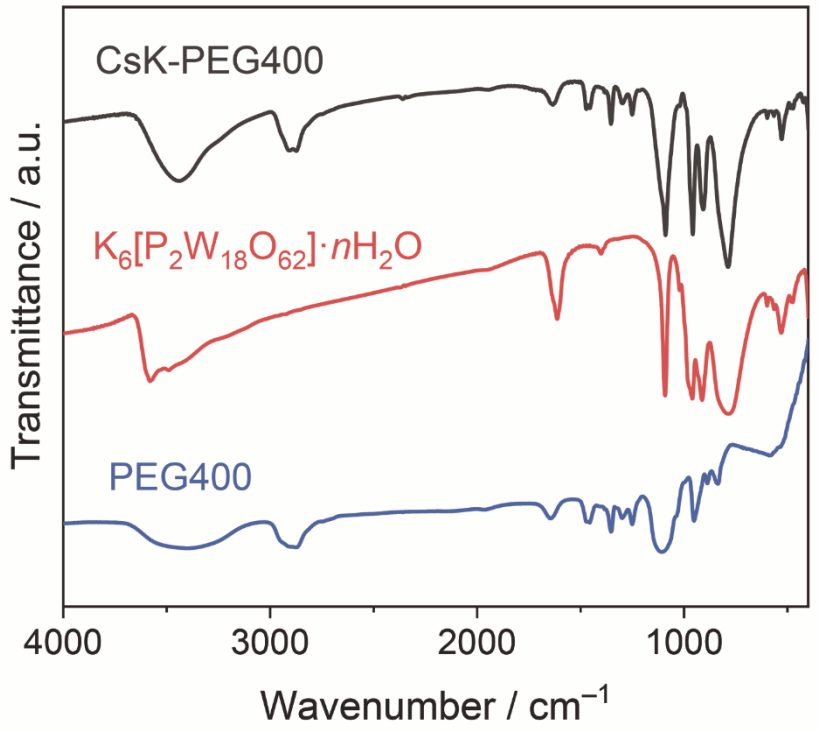

Fig. S1 IR spectra of **CsK-PEG400** (black), $K_6[\alpha\text{-}P_2W_{18}O_{62}]$ (red) and PEG400 (blue).

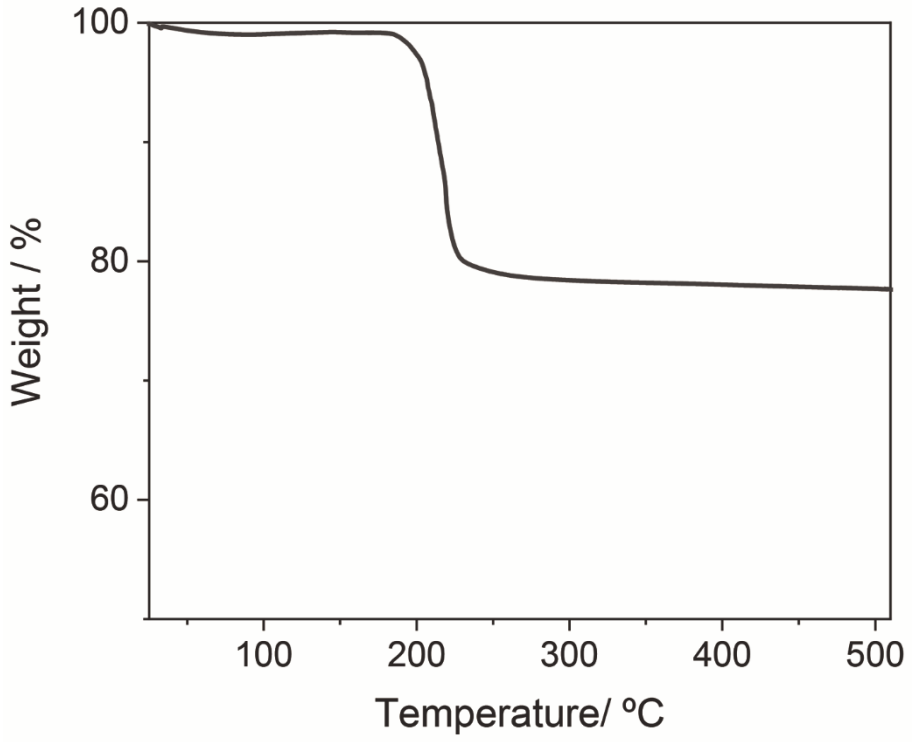

Fig. S2 TGA curve of **CsK-PEG400**.

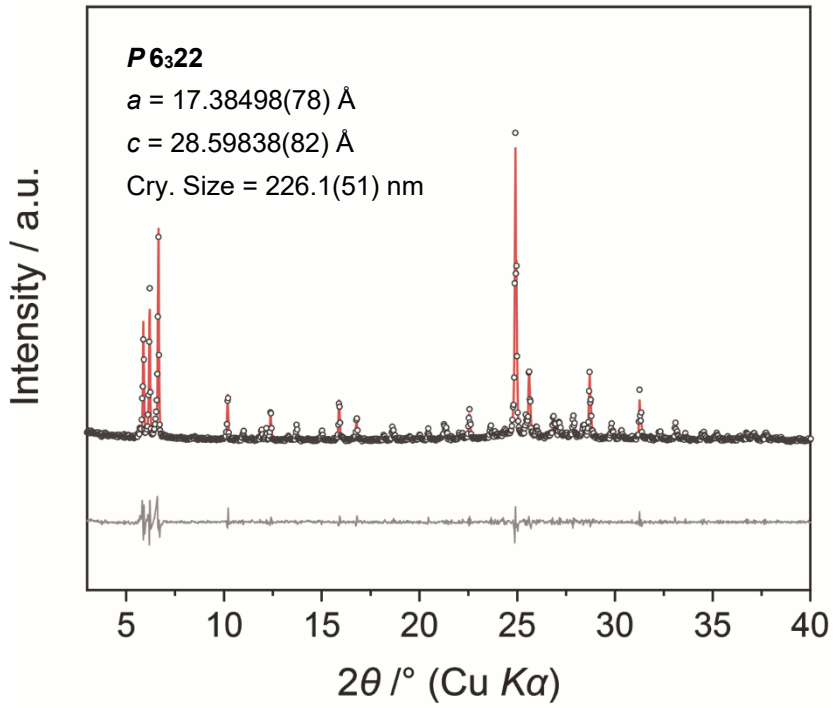

Fig. S3 Experimental (open circles) and calculated (red solid line) PXRD patterns of **CsK-PEG400**. The bottom line shows the difference profile.

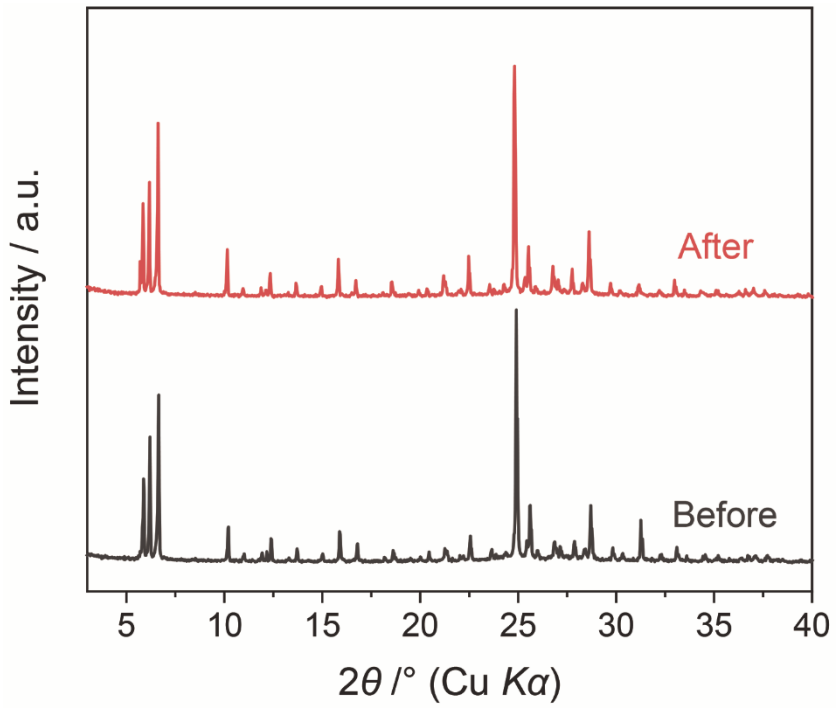

Fig. S4 PXRD patterns of **CsK-PEG400** before and after heating at 150 °C.

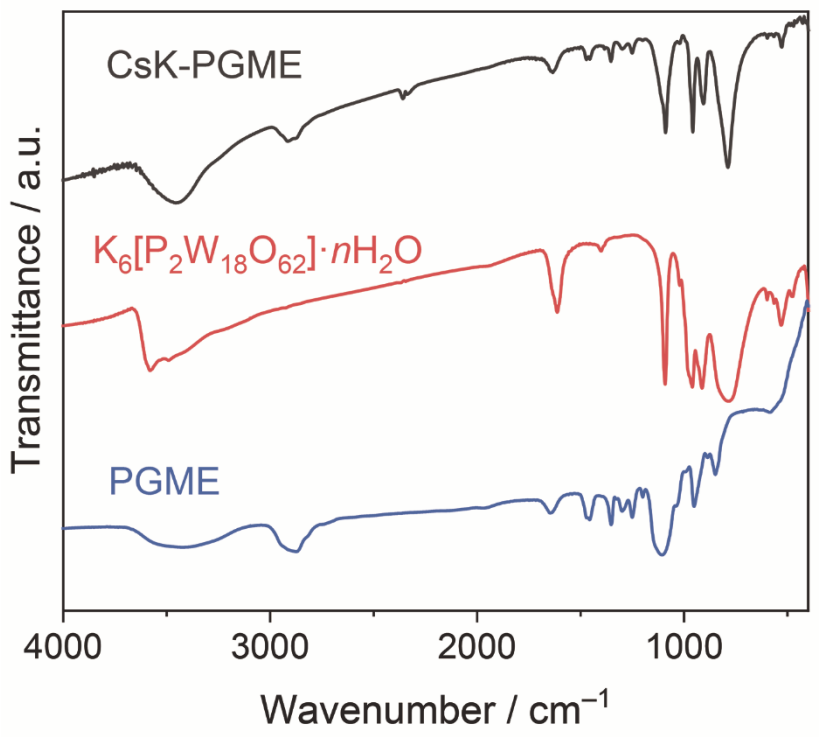

Fig. S5 IR spectra of **CsK-PGME** (black), $K_6[\alpha\text{-}P_2W_{18}O_{62}]$ (red), and PGME (blue).

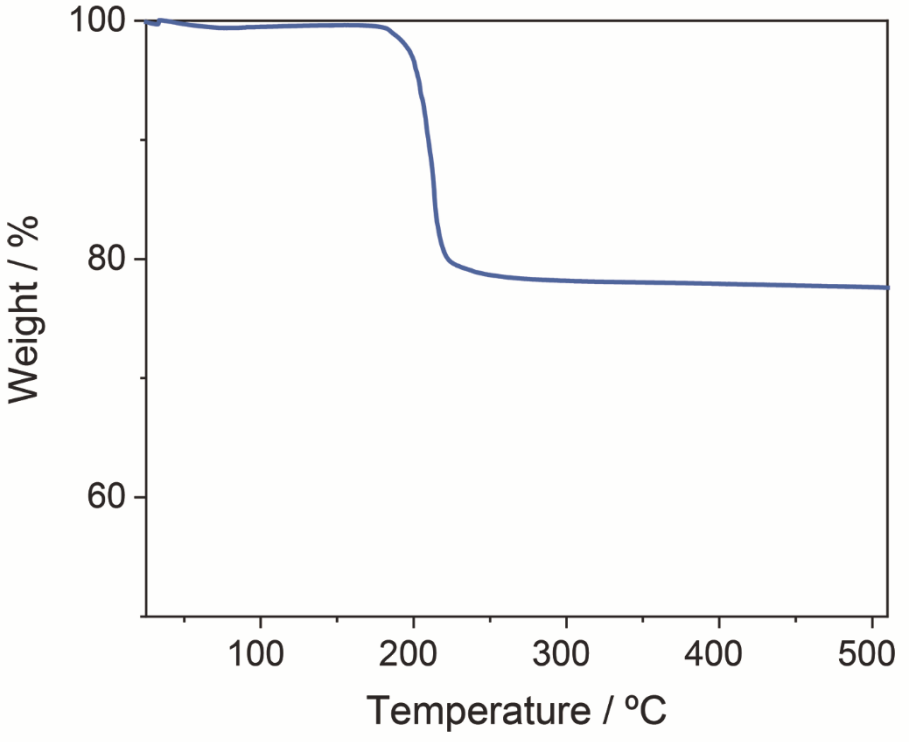

Fig. S6 TGA curve of **CsK-PGME**.

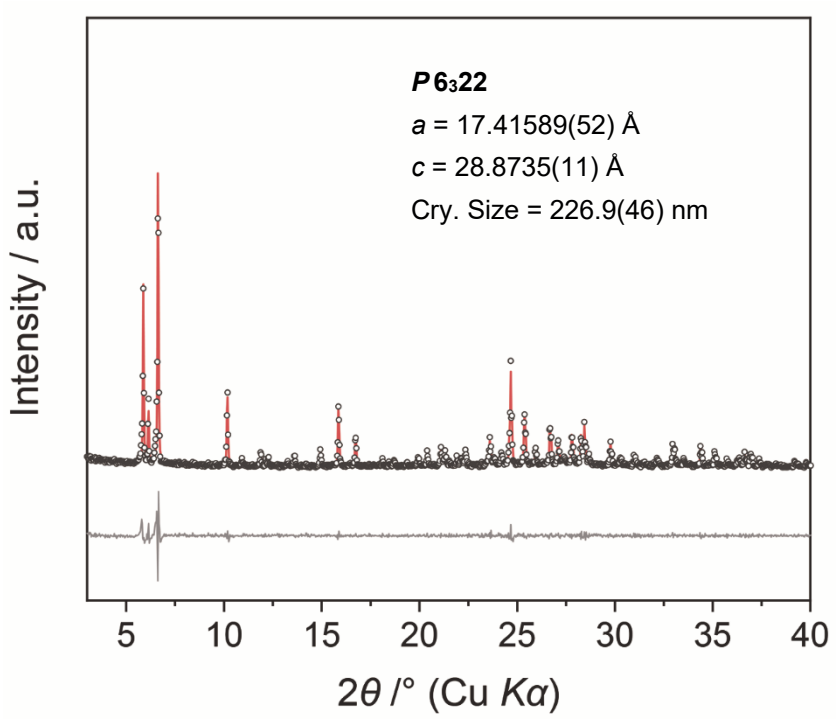

Fig. S7 Experimental (open circles) and calculated (red solid line) PXRD patterns of **CsK-PGME**. The bottom line shows the difference profile.

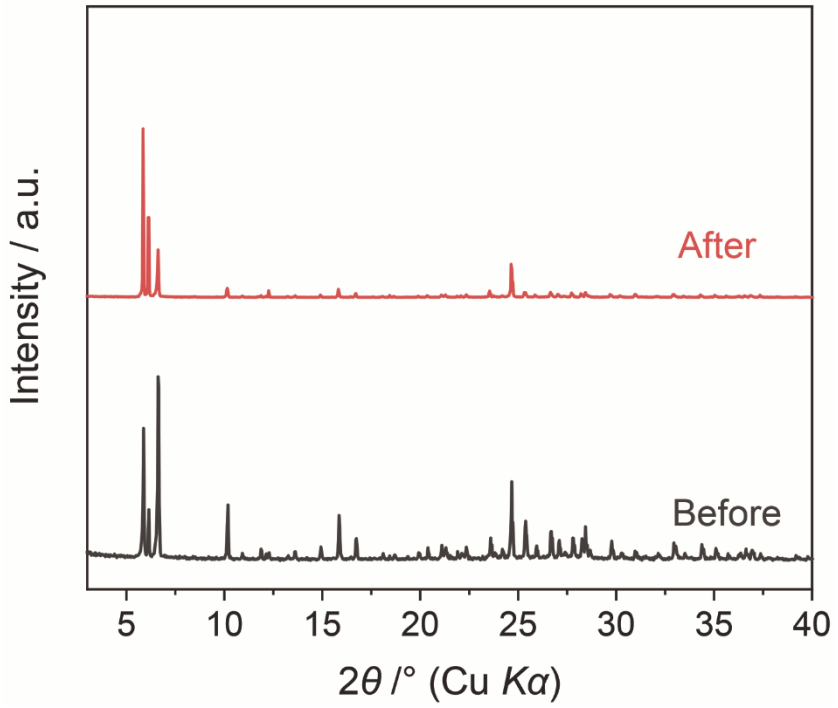

Fig. S8 PXRD patterns of **CsK-PGME** before and after heating at 150 °C.

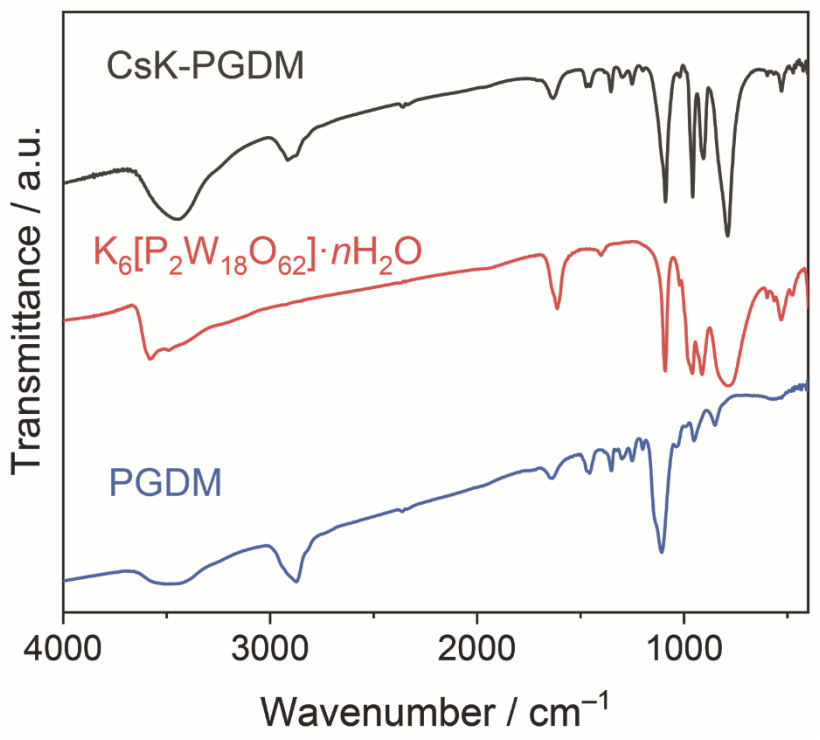

Fig. S9 IR spectra of **CsK-PGDM** (black), $K_6[\alpha\text{-}P_2W_{18}O_{62}]$ (red), and PGDM (blue).

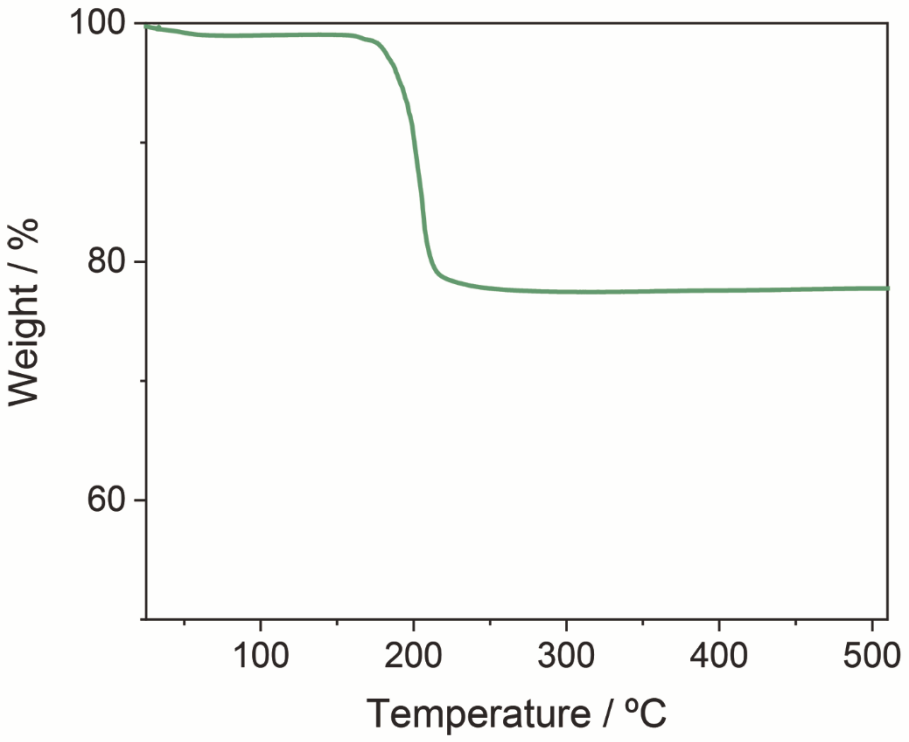

Fig. S10 TGA curve of **CsK-PGDM**.

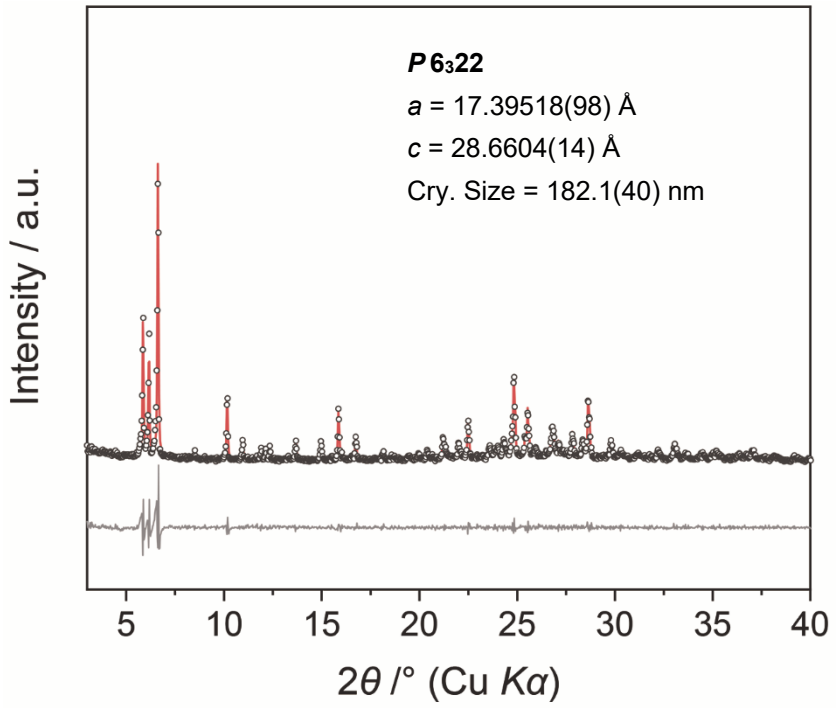

Fig. S11 Experimental (open circles) and calculated (red solid line) PXRD patterns of **CsK-PGDM**. The bottom line shows the difference profile.

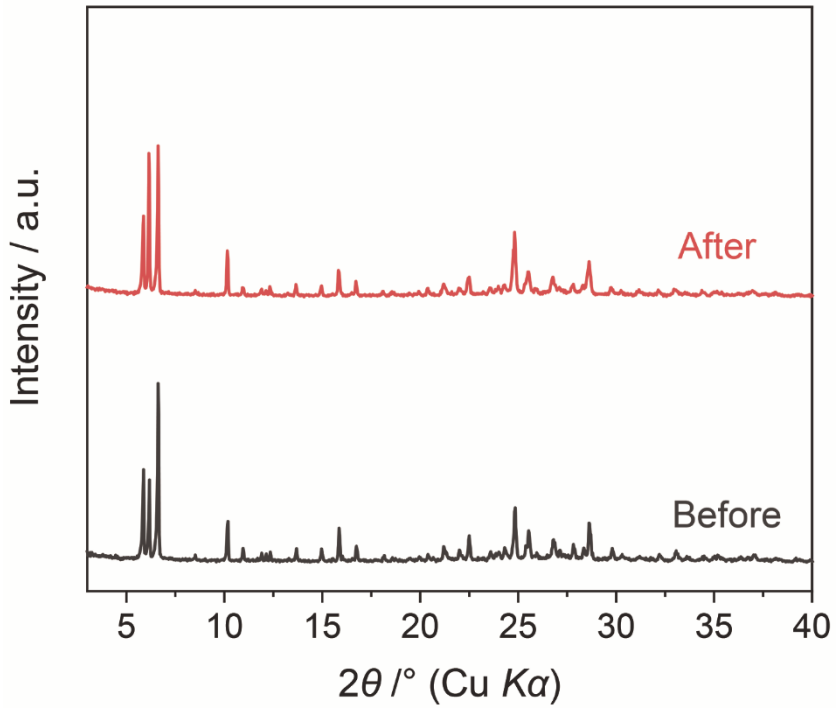

Fig. S12 PXRD patterns of **CsK-PGDM** before and after heating at 150 °C.

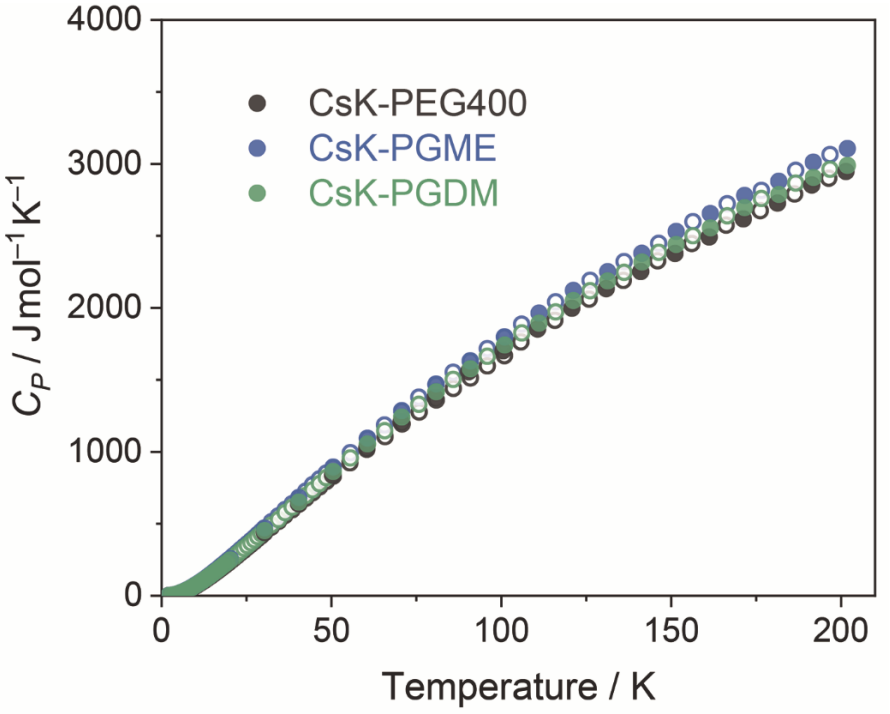

Fig. S13 Specific heat capacities (C_P) of **CsK-PEG400**, **CsK-PGME**, and **CsK-PGDM**.

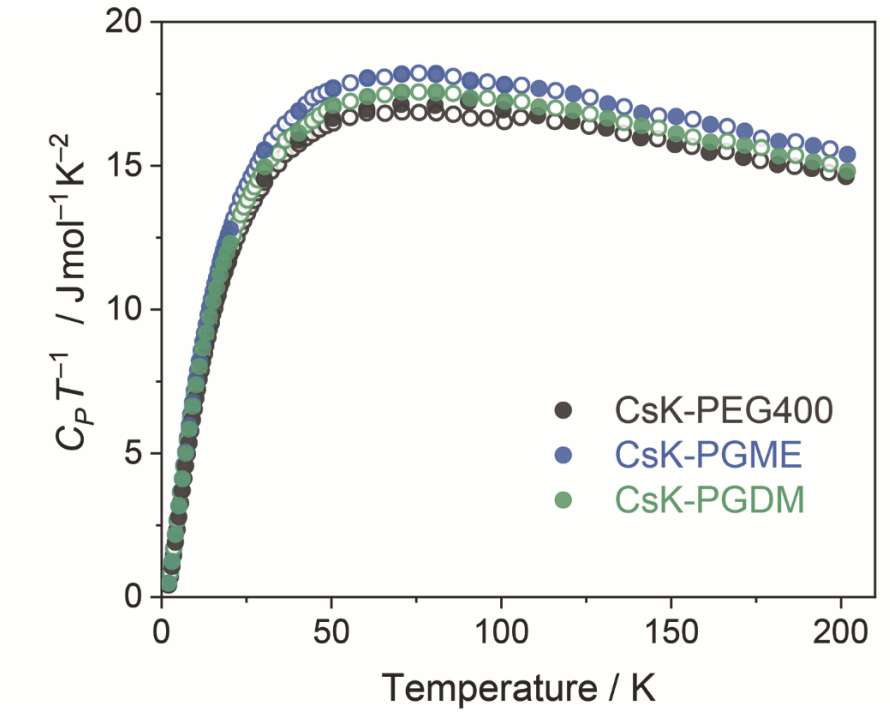

Fig. S14 $C_P\ T^{-1}$ of **CsK-PEG400**, **CsK-PGME** and **CsK-PGDM**.

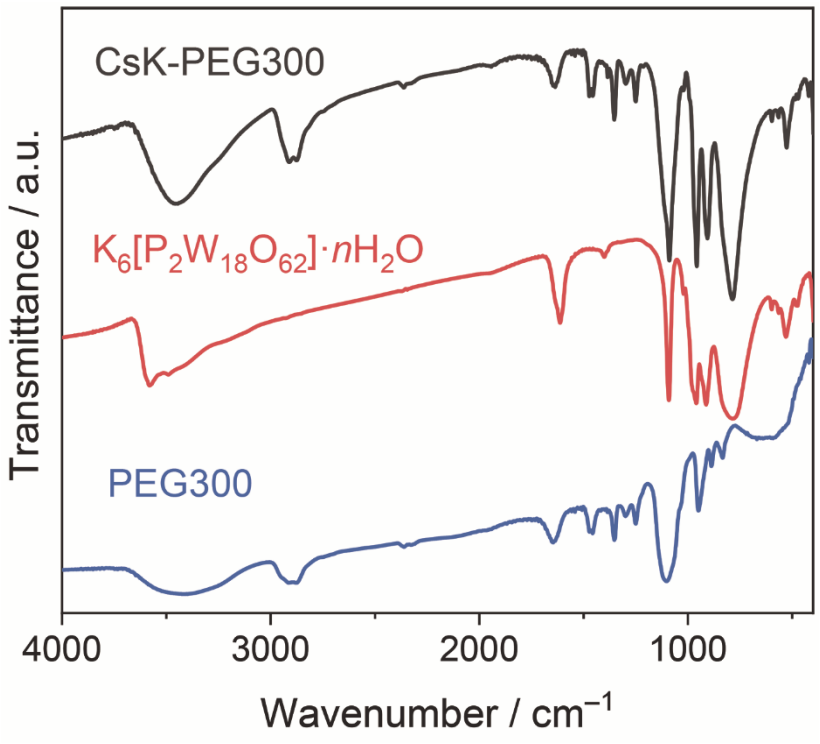

Fig. S15 IR spectra of **CsK-PEG300** (black), $K_6[\alpha\text{-}P_2W_{18}O_{62}]$ (red), and PEG300 (blue).

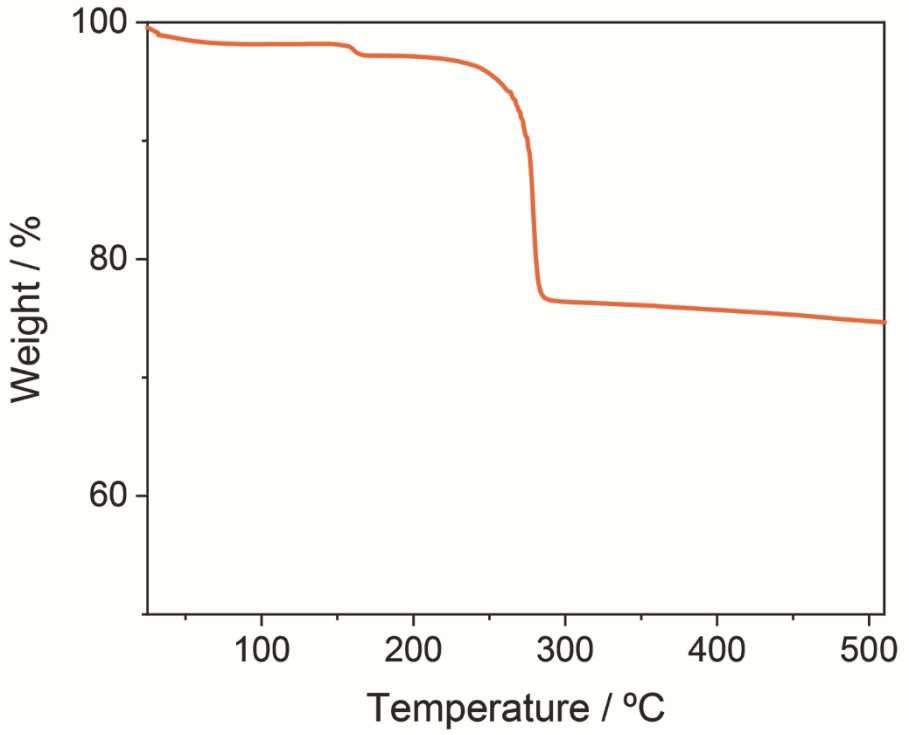

Fig. S16 TGA curve of **CsK-PEG300**.

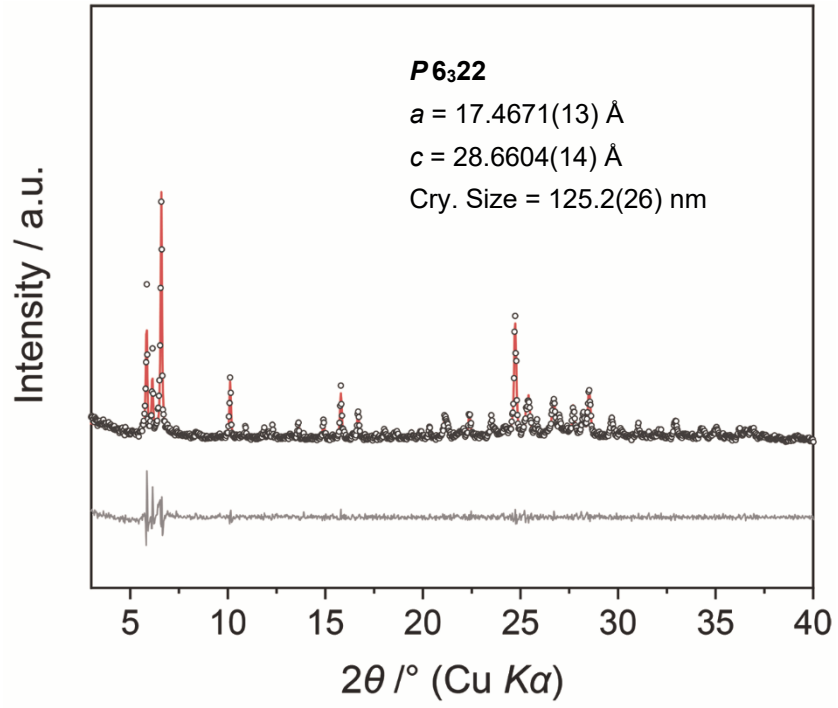

Fig. S17 Experimental (open circles) and calculated (red solid lines) PXRD patterns of **CsK-PEG300**. The bottom line show the difference profile.

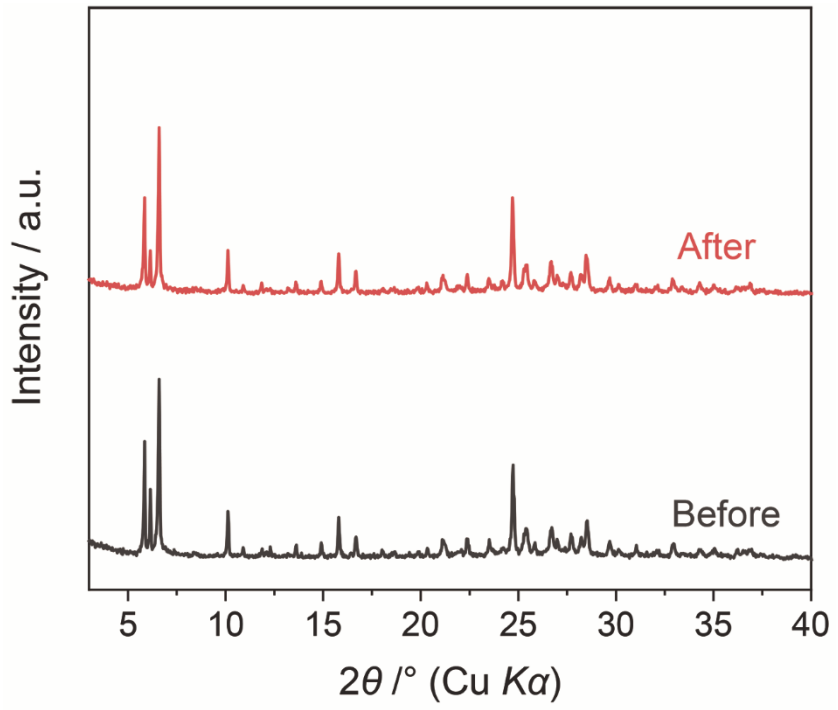

Fig. S18 PXRD patterns of **CsK-PEG300** before and after heating at 150 °C.

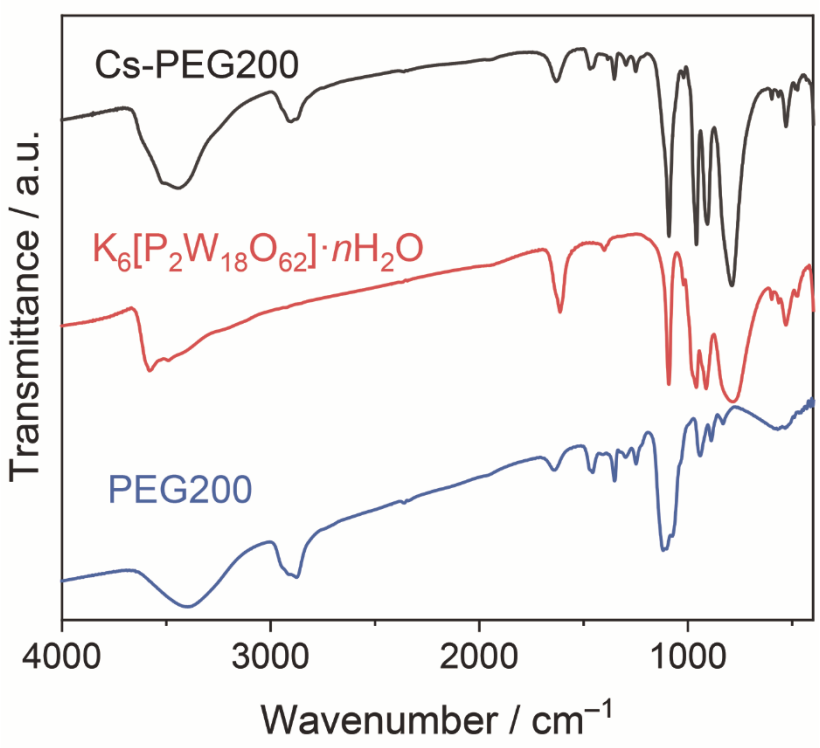

Fig. S19 IR spectra of **Cs-PEG200** (black), $K_6[\alpha\text{-}P_2W_{18}O_{62}]$ (red), and PEG200 (blue).

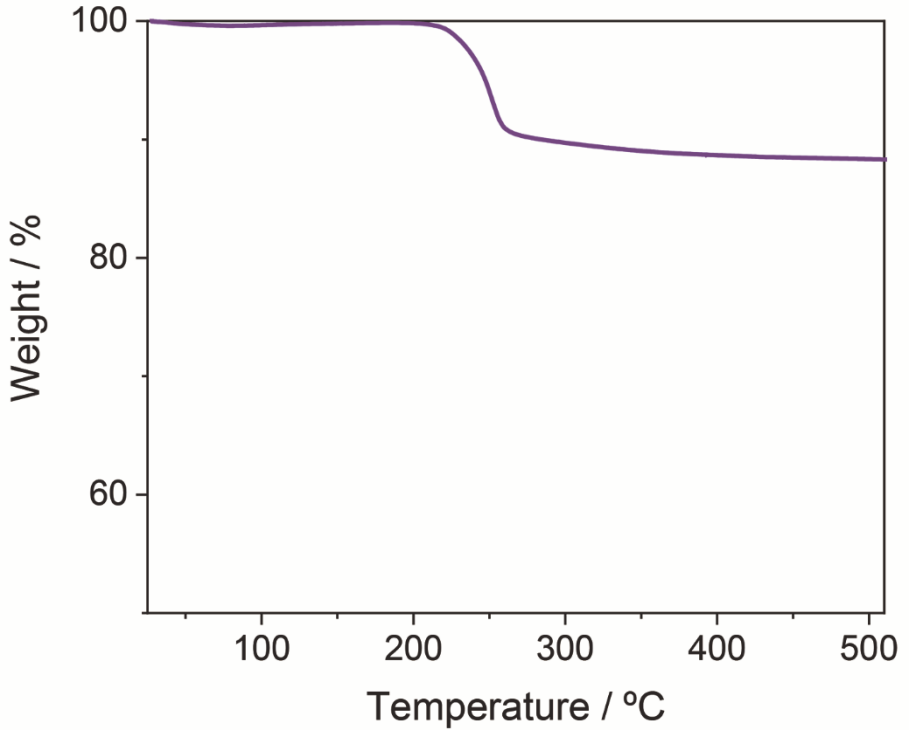

Fig. S20 TGA curve of **Cs-PEG200**.

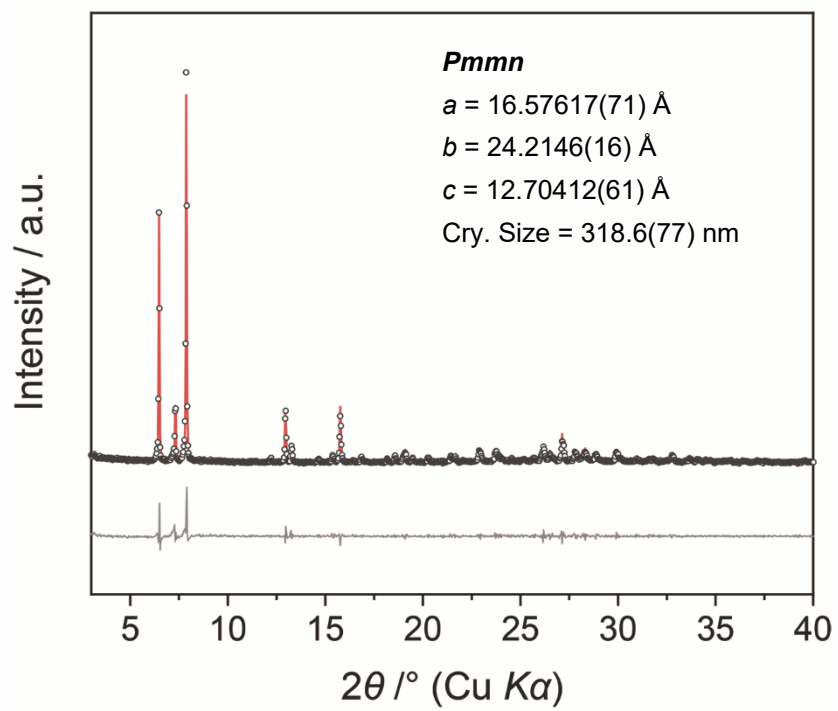

Fig. S21 Experimental (open circles) and calculated (red solid lines) PXRD patterns of **Cs-PEG200**. The bottom line shows the difference profile.

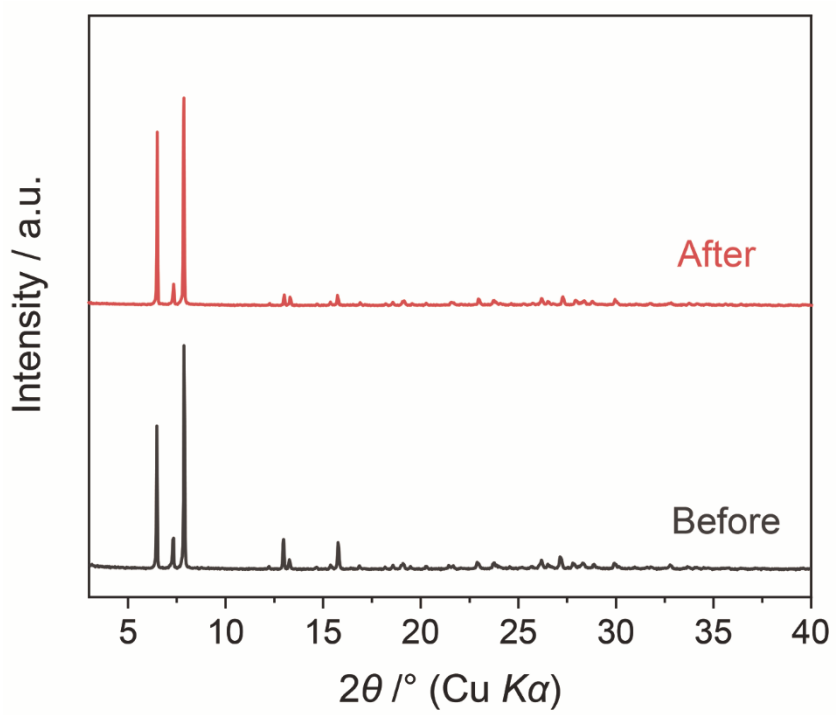

Fig. S22 PXRD patterns of **Cs-PEG200** before and after heating at 150 °C.

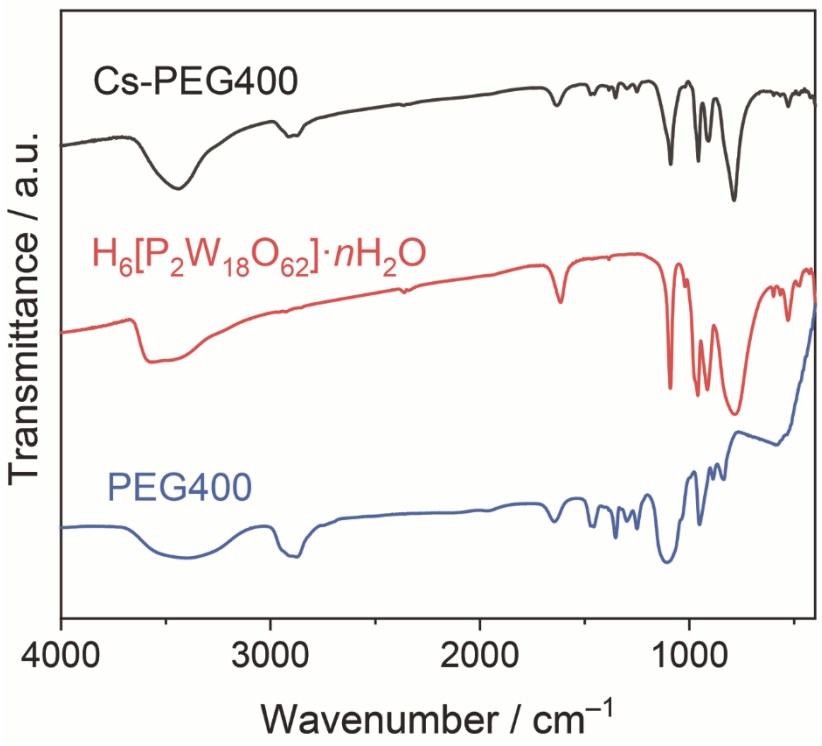

Fig. S23 IR spectra of **Cs-PEG400** (black), $H_6[\alpha\text{-}P_2W_{18}O_{62}]$ (red), and PEG400 (blue).

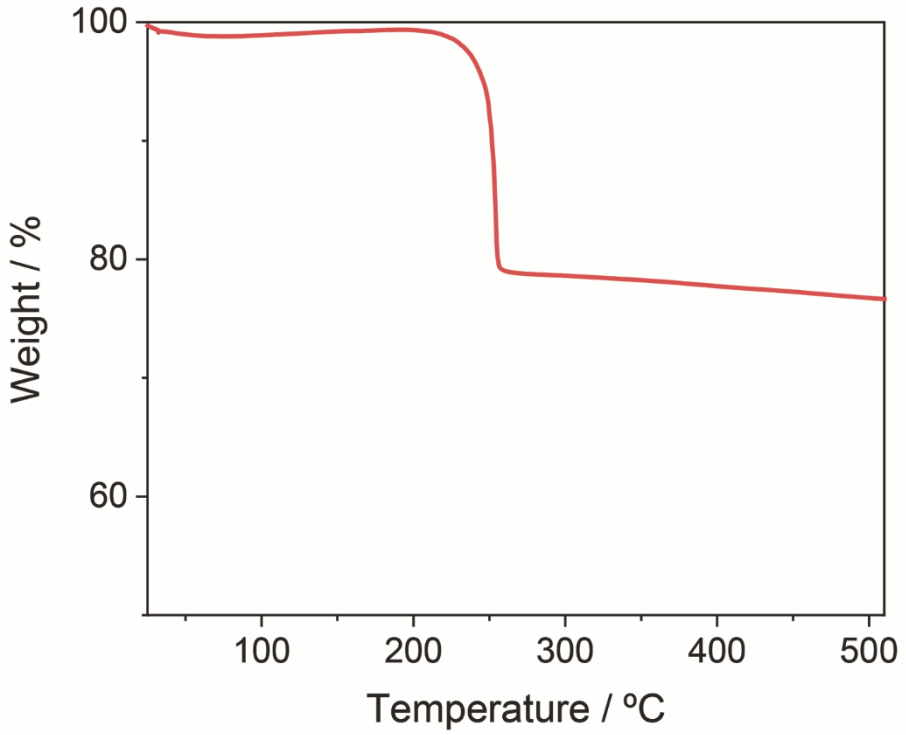

Fig. S24 TGA curve of **Cs-PEG400**.

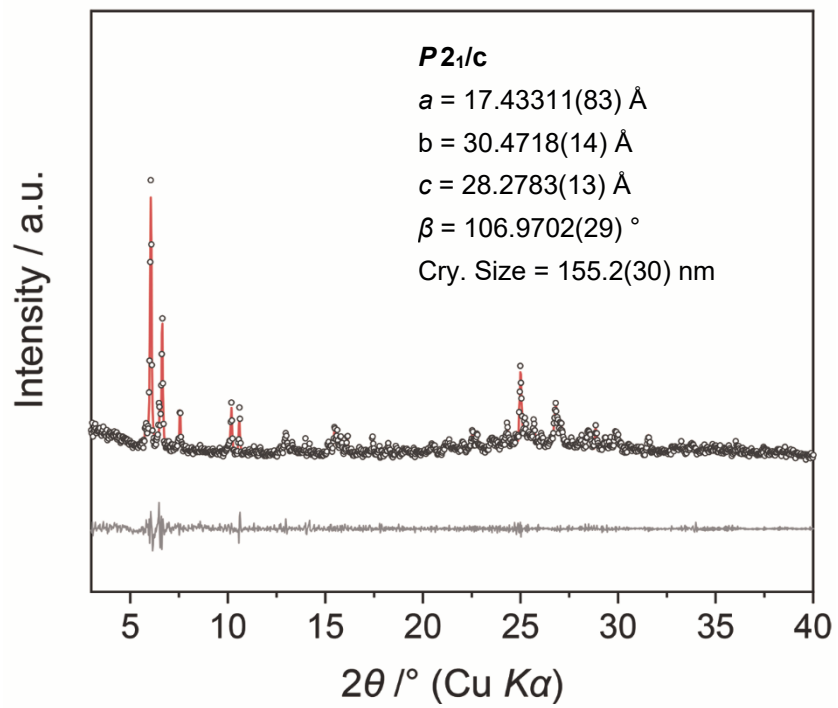

Fig. S25 Experimental (open circles) and calculated (red solid lines) PXRD patterns of **Cs-PEG400**. The bottom line shows the difference profile.

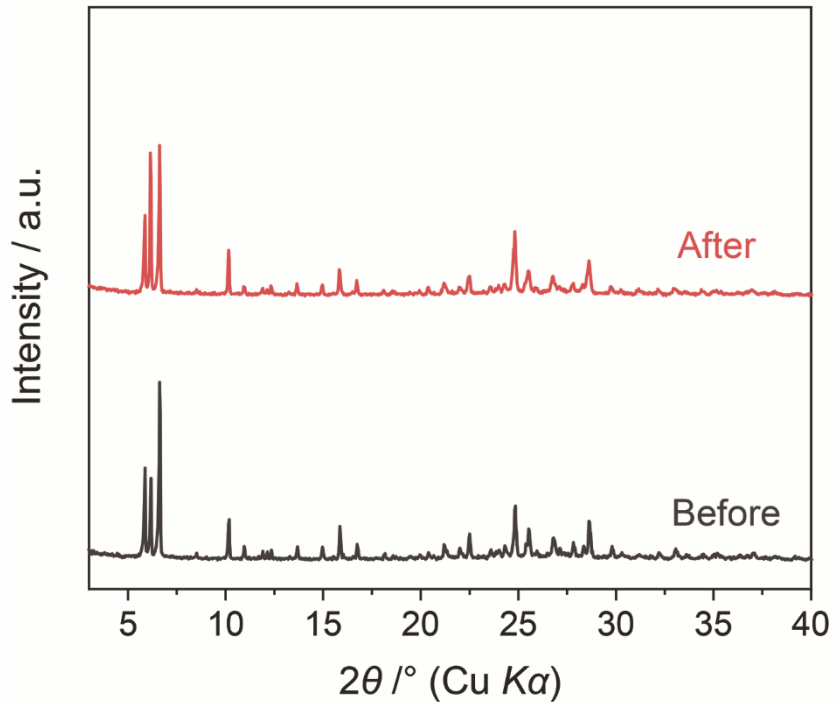

Fig. S26 PXRD patterns of **Cs-PEG400** before and after heating at 150 °C.

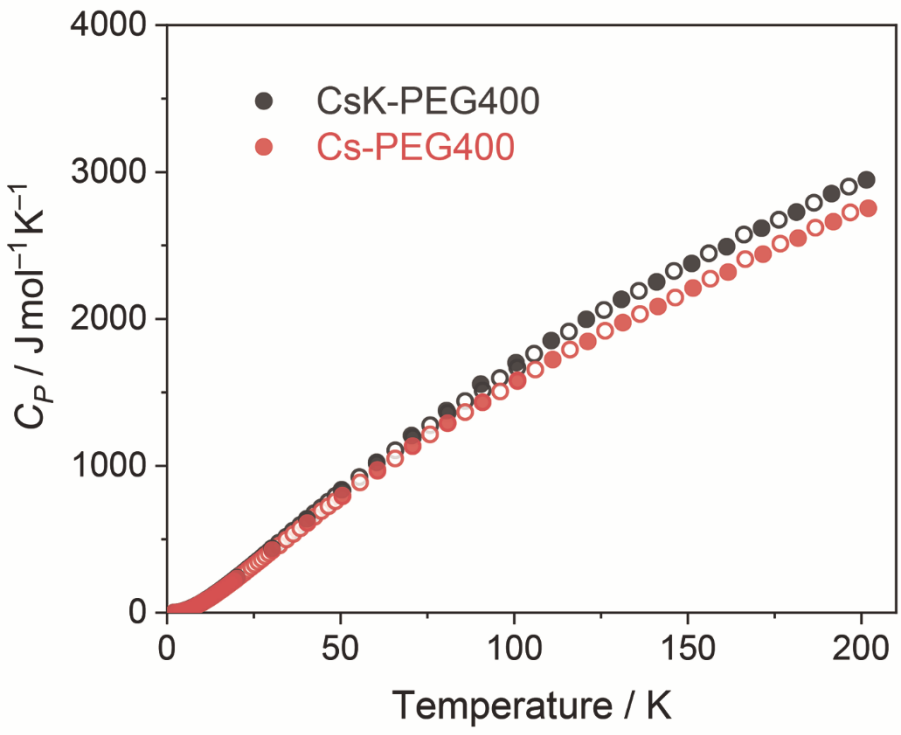

Fig. S27 Specific heat capacities (C_P) of **CsK-PEG400** and **Cs-PEG400**.

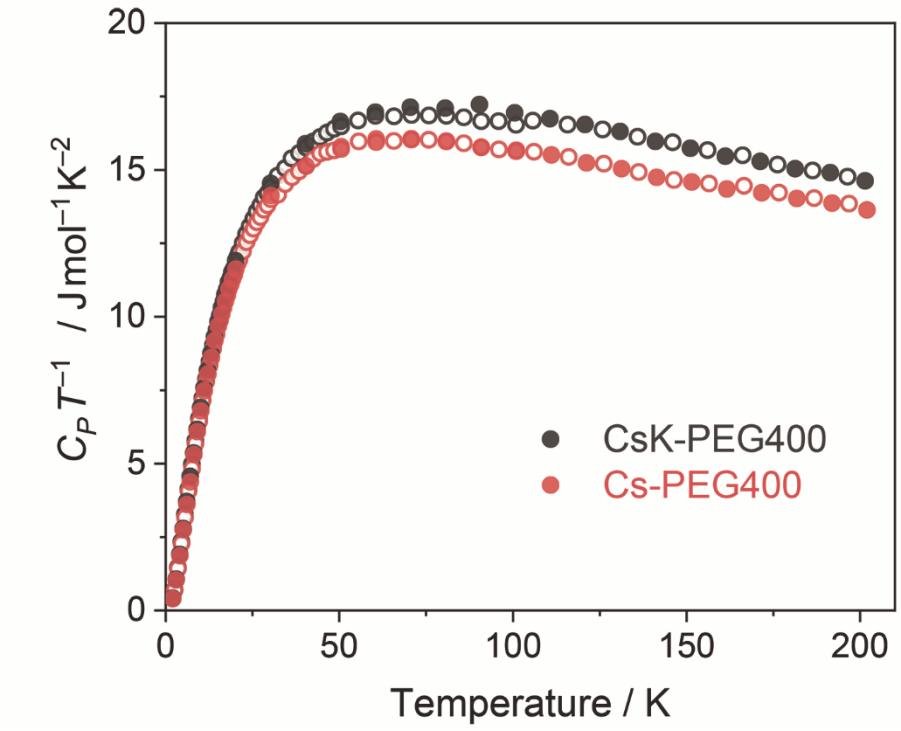

Fig. S28 C_P T^{-1} of CsK-PEG400 and Cs-PEG400.

References

1. (a) C. R. Graham and R. G. Finke, *Inorg. Chem.*, 2008, **47**, 3679–3686; (b) G. Baronetti, L. Briand, U. Sedran and H. Thomas, *Appl. Catal. A*, 1998, **172**, 265–272.
2. W. Minor, M. Cymborowski, Z. Otwinowski and M. Chruszcz, *Acta Cryst.*, 2006, **D62**, 859–866.
3. *CrystalStructure*, ver. 4.*3*; Rigaku Corporation, Tokyo, Japan, 2019.
4. *CrysAlis PRO*, Rigaku Oxford Diffraction, Tokyo, Japan, 2015.